Title page

Title

Proteomics screening post pediatric allogeneic hematopoietic stem cell transplantation reveals an association between increased expression of inhibitory protein FCRL6 on γδ T cells and CMV reactivation.

Running title

Proteomics after pediatric allogenic HSCT

Authors

Adam Alexandersson[1,2,6], Mikko S Venäläinen[3], Nelli Heikkilä[2,7], Xiaobo Huang[2], Mervi Taskinen[1], Pasi Huttunen[1,6], Laura L Elo[3,4], Minna Koskenvuo[1], Eliisa Kekäläinen[2, 5]

Affiliations

1 Division of Pediatric Hematology, Oncology and Stem Cell Transplantation, New Children's Hospital, Helsinki University Hospital, Helsinki, Finland

2 Translational Immunology Research Program, Faculty of Medicine, University of Helsinki, Helsinki, Finland

3 Turku Bioscience Centre, University of Turku and Åbo Akademi University, Turku, Finland

4 Institute of Biomedicine, University of Turku, Turku, Finland

5 HUS Diagnostic Center, Clinical microbiology, Helsinki University Hospital, Helsinki, Finland

6 Children and Adolescents, Pediatric Research Center, New Children's Hospital, University of Helsinki and Helsinki University Hospital, Helsinki, Finland

7 Center of Vaccinology, University of Geneva, Geneva, Switzerland

Corresponding author

Adam Alexandersson

Email: adam.alexandersson@helsinki.fi

Address: Translational Immunology Research Program, PB 21, 00014 University of Helsinki, Finland

Phone: +358522051

Data Sharing Statement

Study protocols and analysis tools will be shared upon reasonable request via email to the corresponding author. Due to the European Union's General Data Protection Regulation (2016/679) we cannot share individual patient data.

ORCID

Adam Alexandersson: 0000-0001-5341-2891

Mikko Venäläinen: 0000-0003-1777-4259

Eliisa Kekäläinen: 0000-0001-6045-108X

Laura Elo: 0000-0001-5648-4532

Minna Koskenvuo: 0000-0002-3796-0991

Nelli Heikkilä: 0000-0002-8879-1569

Xiaobo Huang: 0000-0001-7516-8842

Mervi Taskinen: 0000-0002-9907-4725

Pasi Huttunen: 0000-0002-0731-1245

Financial Disclosure Statement

AA reports funding from the foundations Finska Läkaresällskapet and Lastentautien Tutkimussäätiö. MSV reports funding from the Academy of Finland (grant number 322123). EK reports funding from Lastentautien tutkimussäätiö, University of Helsinki research funds and Helsinki University Hospital Governmental Funding for Research. LLE reports funding from the European Research Council ERC (677943), European Union's Horizon 2020 research and innovation programme (955321), Academy of Finland (310561, 314443, 329278, 335434, 335611 and 341342), and Sigrid Juselius Foundation. LLE's research is also supported by Biocenter Finland, and ELIXIR Finland. XH and PH report no competing financial interests.

Abstract

Objective: Our objective was to study kinetics and associations between inflammation related proteins in circulation after pediatric allogenic hematopoietic stem cell transplantation (HSCT) to reveal proteomic signatures or individual soluble proteins associated with specific complications post HSCT.

Methods: We used a proteomics method called Proximity Extension Assay to repeatedly measure 180 different proteins together with clinical variables, cellular immune reconstitution, and blood viral copy numbers in 27 children aged 1-18 years during a two-year follow up after allogenic HSCT. Protein profile analysis was done using unsupervised hierarchical clustering and a regression-based method, while Bonferroni-corrected Mann-Whitney U test was used for time point specific comparison of individual proteins against outcome.

Results: At 6 months after allogenic HSCT, we could identify a protein profile pattern that was associated with occurrence of the complications chronic graft-versus-host disease, viral infections, relapse, and death. When protein markers were analyzed separately, the plasma concentration of the inhibitory and cytotoxic T cell surface protein FCRL6 (Fc receptor-like 6) was higher in patients with CMV viremia (log2-fold change 1.5 (p=9.9 x 10-4), 2.5 (p=3.5 x 10-4) and 2.2 (p=0.045) at time points 6, 12 and 24 months). Flow cytometry confirmed that FCRL6 expression was higher in innate-like T cells, indicating that these cells have a role$\gamma\delta$ in controlling CMV reactivation in HSCT recipients.

Conclusions: The potentially druggable FCRL6 receptor on cytotoxic T cells appears to have role in controlling CMV viremia post-HSCT. Our results suggests that system level analysis is a useful addition to the studying of single biomarkers in allogeneic HSCT.

Introduction

Allogenic hematopoietic stem cell transplantation (HSCT) has the potential to cure several malignant and benign conditions of the bone marrow, but is burdened by risk of complications[1]. Routinely used clinical parameters and laboratory tests are insufficient to predict the occurrence of potentially lethal and debilitating complications such as graft-versus-host disease (GVHD)[2] and bacterial, fungal and viral infections[3–5]. Reactivation of latent cytomegalovirus (CMV) is one of the main complications after allo-HSCT and an independent risk factor for chronic GVHD, the main cause for long-term morbidity after HSCT. Tools to predict complications are needed since for example antivirals used to treat CMV reactivations are potentially toxic, and their use should be limited only to patients that clearly benefit from them.

Many studies have focused on predicting CMV reactivation but validated biomarkers are still lacking[6]. Delayed immune reconstitution is associated with CMV reactivations[6]. CMV-specific CD8+ T-cell cytokine signatures can predict the risk of CMV reactivation, but testing of cellular responses is complicated and not suitable for routine clinical laboratories[7]. Testing for individual biomarkers or a panel of soluble plasma biomarkers to predict complications after HSCT would better suit clinical practice. Proteomics approaches after HSCT and results are promising regarding understanding of pathogenesis as well as predicting relapse, non-relapse mortality, acute GVHD (aGVHD) and chronic GVHD (cGVHD), including therapy response[2,8,9]. No biomarker or panel of biomarkers is, however, yet widely in clinical use[2].

A benefit of the proteomics and other systems immunology approaches is their hypothesis-generating attribute, as opposed to testing a priori formulated research questions[10]. To our knowledge, no similar proteomic studies have been performed prospectively on children receiving HSCT with myeloablative conditioning. In order to better predict the onset and to understand mechanisms of severe complications after HSCT in children, we performed a longitudinal deep analysis on the plasma proteome in relation to clinically relevant outcomes like cGVHD, viral infections, relapse and death.

Materials and methods

Patient cohort, sample collection and clinical outcomes

This single-center study from the New Children's Hospital, Helsinki University Hospital, Finland, followed 27 children with hematological cancer aged 1-18 years for two years after HSCT with myeloablative conditioning. We have earlier published the cohort's clinical characteristics, including timing of complications[11]. In addition to registering clinical disease- and transplant-related features, symptoms and signs, we collected blood samples at time points 3, 6, 12 and 24 months post HSCT. Plasma was isolated and stored frozen. Peripheral blood mononuclear cell (PBMC) isolation was done with gradient centrifugation (Ficoll-Paque PLUS, Cytiva, MA, the USA) and cells were frozen in 10% DMSO in fetal-calf serum and stored frozen in liquid nitrogen or -140°C. We measured viral copy numbers of CMV, human herpesvirus 6 (HHV6), BK virus (BKV) and Epstein-Barr Virus (EBV) at 3, 6, 12 and 24 months, and additionally extracted levels of the same viruses from the patient records, when they had been requested by the clinician. Immune reconstitution (IR) was followed with clinical lymphocyte subtype testing (total CD3+ T cells, CD4+ T helper cells, CD8+ cytotoxic T cells, CD19+ B cells and NK cells). Lymphocytes and subclasses were quantified using accredited flow cytometry for clinical use and viral levels with real-time PCR at an accredited clinical laboratory (HUS Diagnostic Center, Helsinki, Finland). Quality control and descriptive statistics are found in the supplementary material.

Since the spectrum of HSCT complications is diverse and numerous outcome subgroups strain statistical analyses, we created a composite outcome called "complication free". Complication-free status was attributed to patients who did not suffer any of the following: death during follow-up, relapse during follow-up, cGVHD as per the 2014 NIH criteria[12], aGVHD grade 3 or 4[13], CMV viremia, BKV viremia over 10 000 IU/ml, HHV6 viremia in combination with BKV, or EBV viremia. "Complication-prone" status was correspondingly designated if any of the above findings were present during the follow-up.

The study was approved by the Ethics Committee of the Helsinki University Hospital (HUS/2306/2016), and written informed consent was obtained from all parents and patients above 6 years of age. Baseline demographics are presented in Table 1.

Proteome analysis

For proteome analysis we used the Proximity Extension Assay (Olink, Uppsala, Sweden) on freshly thawed frozen plasma samples at time points 3, 6, 12, and 24 months post-HSCT. In short, Proximity Extension Assay is a proteomics method where two target-specific oligo-conjugated antibodies bind their respective epitopes that are very closely situated on the target, allowing the oligos to hybridize. After this, only the hybridized oligonucleotide sequences are detected with qPCR. The method is highly specific and enables a relative quantification of large amounts of protein targets simultaneously in a longitudinal sample series[14]. We used two Olink panels ("Inflammation" and "Immune response") consisting of 92 proteins each (supplementary material, Table S1). The Olink analysis service was provided by the Biomedicum Functional Genomics Unit at the Helsinki Institute of Life Science and Biocenter Finland at the University of Helsinki.

Flow cytometry

For FCRL6 flow cytometric analysis, PBMCs from 17 patients collected at 3, 6, 12, and 24 months post-transplantation were used as available (supplementary material, Table S2). Frozen aliquots of PBMCs were thawed in +37°C water bath and transferred to 50 mL conical tubes. Then, 10 mL of +37°C thawing solution (RPMI supplemented with 10% CTL-WASH (Cellular Technology Limited) and 10 ug/mL DNase I) was added slowly, the tube was centrifuged at 350g, 10min in room temperature, and the supernatant was discarded. Cells were washed again with 10mL of thawing solution at 350g for 10 min, adjusting the temperature to +4°C during the centrifugation and resuspended in +4°C staining buffer (PBS supplemented with 10% FCS and 10mM EDTA).

For each individual, 1-2 million cells were washed with 500 ul of staining buffer. The fluorescent-labeled anti-human antibodies are listed in Table S3. The optimal staining concentrations for antibodies were titrated with live PBMCs. Cells were incubated with a mix of antibodies and 1:1000 LIVE/DEAD Fixable Green Dead Cell Stain (Thermo Fisher) diluted in Brilliant Stain Buffer (BD Biosciences) in a final volume of 50 ul for 30 min in +4°C. Cells were washed with 1 mL of staining buffer and run on LSR II Fortessa (BD Biosciences). A median of 78 000 (range 8 000-990 000) viable lymphocytes were registered per each run. Flow cytometric data was analyzed using FlowJo software (version 10.8, BD, Biosciences) using fluorescence-minus-one staining for FCRL6 expression, and biological negative controls when applicable. The full gating strategy is displayed in the supplementary material, Figure S1.

Statistical methods

Protein concentrations were expressed as Normalized Protein eXpression (NPX) values, an arbitrary unit on log2-scale. Values below qPCR limit of detection (LOD) were treated both by using actual obtained data and, due to the risk of bias and the risk of missing out on relevant associations, by setting values below LOD to missing. However, proteins with over 50% of measured values below LOD were excluded completely from further analyses. The multidimensional protein data was visualized by applying principal component analysis (PCA, supplementary material, Fig. S2) on data at each individual time point. Time-course trends of individual proteins were visualized using sparkline plots generated by applying Loess regression smoothing for complication-free and complication-prone groups.

Unsupervised hierarchical clustering of protein levels was performed using the Euclidean distance and Ward's method independently at each time point. Prior to clustering, the NPX values were scaled using z-score normalization. Differences in outcome rates between identified clusters were compared using the chi-squared or Fisher's exact test (n<5). Differences in trends of immune reconstitution between the clusters over time were analyzed

using linear mixed effect models with cluster, time and cluster×time interaction term as fixed effects and including a random intercept for patients.

Global correlation matrices were computed and prepared for visualization using R package DGCA (https://pubmed.ncbi.nlm.nih.gov/27846853/). For each time point, the top ten protein pairs with the greatest absolute difference in correlation between complication-free and complication-prone patients were reported. Differentially correlating protein pairs were identified using R package DiffCorr (https://pubmed.ncbi.nlm.nih.gov/23246976/).

Differentially expressed markers for outcomes of interest were identified using maSigPro, a regression-based method designed for identifying differential expression profiles between experimental groups in time-course experiments[15]. Here, up to third degree polynomial models were considered and the obtained p values were corrected for multiple comparisons by applying the Bonferroni correction. For each model, we used $R^2=0.5$ as a threshold for acceptance into the group of significant proteins. Additionally, differential expression for outcomes of interest at each individual time point was tested using Bonferroni-corrected Mann-Whitney U test.

All statistical analyses and modeling were carried out using the R statistical computing environment version 4.0.3 (R Core Team, 2016. R: A language and environment for statistical computing. R Foundation for Statistical Computing, Vienna, Austria. URL https://www.R-project.org/). The level of significance was set at $p<0.05$.

Results

Unsupervised clustering of plasma proteome identifies patients with HSCT-related complications and poor immune reconstitution

As depicted in the sparkline plots (Fig. 1), individual protein levels plotted over time showed that almost all measured proteins changed over time with varying patterns in complication-free and complication-prone individuals. Therefore, we decided to first investigate a possible association between a global plasma protein profile and clinical outcome measures, by

performing an unsupervised clustering. A heatmap (Fig. 2A), created using hierarchical clustering based on protein levels at 6 months post-HSCT, revealed two clusters with distinctly different outcome profiles. Similar but less clearly separating pattern for two main clusters was visible in other timepoints (supplementary material, Fig. S4). We chose to focus on the 6 month time point in the following analyses, since by this time most of the complications had occurred, but the reconstitution of the immune system would not yet be finalized. At this point, all aGVHD had occurred, every viral infection was diagnosed[11] and most cases of cGVHD had begun. Some cases of death and relapse had yet to occur, but all patient-specific complications were registered and included in analysis independent of time of onset, since relevant immunological patterns might be seen before, during, and after debut.

At 6 mo after HSCT, complication-prone status was clearly more frequent in cluster 2, where 14/15 patients had complication-prone status vs. 4/10 in cluster 1 (93% vs. 40%, p=0.007 by Fisher's exact test). Of individual complications, the separation was mainly explained by higher CMV infection incidence in cluster 2 (53% vs. 10%, p=0.04) as well as the major complications of relapse, death, and cGVHD only occurring in cluster two. Other viral reactivations were distributed evenly in both clusters: HHV-6 reactivation affected 40% of the patients in cluster 2 vs. 20% in cluster 1 (p=0.4 by Fisher's exact test), EBV and BKV viremias occurred with similar frequencies (13% vs. 30% (p=0.4) and 47% vs. 50% (p=1.0), respectively). The frequencies of aGVHD were similar (67% vs. 60%, p=1.0), but the clinically more relevant aGVHD grades 3 and 4 were trending to be more common in cluster 2 (23% vs. 10%, p=0.6). Corresponding heatmaps for other timepoints also showed association with major clinical outcomes (supplementary material, Fig. S4).

We next analyzed how these two clusters differed in their overall cellular immune reconstitution parameters. Numbers of T cells (defined as CD3+CD19-), CD4+ T cells (defined as CD3+CD19-CD4+), and B cells (defined as CD3-CD19+) in the circulation were significantly lower from 6 mo time point onwards in the complication-enriched cluster 2 when the whole follow-up was included in the statistical analysis (Fig 2B). In cluster 2, total T cells and CD4+ T cells were lower from time point 6 months onwards, B cells during the whole

follow-up. Interestingly, CD8 T and NK cell counts did not show differences. We thus can conclude that follow-up-wide immune reconstitution of CD4 T cells and B cells correlated with protein profile status at the 6-month time point (Fig. 2B).

In all, our unsupervised analysis highlighted that CMV reactivation was one of the most defining clinical features for the patients segregated by a specific plasma inflammatory proteome profile. Moreover, this proteome profile was evident prior to failure in specific parts of cellular immune reconstitution.

Protein coexpression levels are connected to outcome

We analyzed the global evolution of the proteome profile by studying patterns of correlating proteins between our complication-free and complication-prone groups (Fig. 3A-B). Positive and negative correlation coefficients respectively indicate a correlated upregulation or a correlated downregulation of two proteins whereas a correlation coefficient around 0 indicates no coordinated expression of two proteins. The complication-prone patients had a narrow distribution of correlation coefficients peaking at 0 indicating little protein coexpression in early timepoints of 3 and 6 months when compared to complication-free patients. On the contrary, complication-free patients had a positively skewed pattern of correlation coefficients indicating correlated, i.e. coordinated, upregulation of proteins (Fig. 3A). At 12 months after HSCT, at peak thymopoiesis, the protein correlations of the complication-prone patients become positively skewed while complication-free patients had an even Gaussian distribution of the correlation coefficients, reflecting the homeostasis acquired (Fig. 3A). This is illustrated in the correlation matrix of different correlations between proteins: At the early timepoints in the complication-free patients there is a clear module of coexpressed proteins while in complication-prone patients the protein expression is disorganized. In contrast at 12-months-time point, modules of coexpressed proteins were observed only in the complication-prone patients (Fig. 3B).

In summary, the protein correlation patterns over the immune reconstitution period after HSCT are different depending on the outcome. Graphically, the Pearson's correlation

matrices show that patients with more complications have less correlating protein pairs, i.e. a more random protein profile at early time points. This was also shown statistically (supplementary material, Table S4), where protein pair correlation level was higher in the complication-free compared to the complication-prone group at early time points. The positively skewed protein correlation pattern in complication-prone individuals one year after HSCT could indicate that achieving immune homeostasis was delayed in the complication-prone individuals.

Individual protein trajectories are associated with specific outcomes

Our analysis thus far has established that our complication-free and complication-prone patients had qualitatively different proteome profiles over the immune reconstitution after allo-HCST. Because large-scale proteome analysis is not feasible for use in clinical practice, we continued to analyze specific proteins in relation to specific outcomes over the whole course of our prospective sample set. Here, we applied the maSigPro regression-based analysis which follows a two steps regression strategy to find protein expression values with significant temporal expression changes. We reasoned that the proteins with significantly different expression values during the whole immune reconstitution period have the highest potential to be clinically relevant biomarkers. In addition, we tested the protein levels against clinical outcomes at every time point using the Mann-Whitney method in order to identify the clinical correlates for each identified potential biomarker (Fig. 4).

Our analysis with maSigPro showed that proteins CLEC4A (C-type lectin domain family 4 member A), AREG (Amphiregulin), OPG (osteoprotegerin, also known as tumour necrosis factor receptor superfamily member 11B) and FCRL6 (Fc Receptor Like 6) levels showed significantly different expression values over the whole immune reconstitution (Fig. 4A). When we correlated these proteins with clinical outcomes, we found correlations between cGVHD and low CLEC4A (also known as DCIR [DC immunoreceptor], $p=3.73 \times 10^{-12}$), high AREG ($p=2.19 \times 10^{-15}$) and high OPG ($p=3.85 \times 10^{-13}$) (Fig 4A). Moreover, there was a highly significant association between CMV viremia and high FCRL6 ($p=3.18 \times 10^{-18}$) (Fig. 4A).

Of the proteins that were significantly different over the whole follow-up period, FCRL6 showed the clearest connection with outcome: for CMV infection at time points 6, 12 and 24 months, log2-fold change was 1.52 ($p=9.9 \times 10^{-4}$), 2.47 ($p=3.5 \times 10^{-4}$) and 2.25 ($p=0.045$) (Fig 4B). In time point specific analysis, CMV viremia was also associated with high CCL23, high KLRD1, high IL12RB, and high CD8A but these correlations were statistically significant in only one or two timepoints and the fold-change differences lower than with FCRL6 (Fig 4C). For example, higher CCL23 expression levels were significantly associated with CMV reactivation only in the earliest timepoint, after which its expression trajectory was not significantly different from the individuals who did not have CMV reactivation. Only FCRL6 showed significant differences in all time points from the 6-month timepoint onwards. On the other hand, overall complication-prone status was associated with high MMP-1 and low CCL3 (C-C motif chemokine ligand 3, also known as macrophage inflammatory protein 1 alpha). These two proteins, which are known pro-inflammatory molecules, appeared to be indicative of a successful immune reconstitution.

γδ T cells expressing FCRL6 associates with CMV infection

FCRL6 appeared to be the most significant protein differentiating complication-free and complication-prone patients from 6 months after HSCT onwards. Since it was associated with CMV reactivation, we used flow cytometric analysis to further focus on its expression on cytotoxic T cells with known roles to control CMV. Overall, there was a higher trend for FCRL6 expression in CD8+ T cells in patients with CMV viremia than in those without, but the results remained statistically nonsignificant (Fig. 5A). No statistically significant differences of FCRL6 expression between patients with or without CMV viremia were observed in effector-memory, central memory or RA+ effector-memory subsets of CD8+ T cells except for a slight difference at 12-month-time point for central memory subset. We then concentrated on another cytotoxic T cell population, the γδ T cells (defined as CD3+CD8+gamma-delta+), where we observed significantly higher levels of FCRL6 expression in CD8+ γδ T cells on timepoints 6 and 12

months post-HSCT in patients with CMV viremia (Fig. 5B). In addition, the expression of FCRL6 in all γδ T cells was significantly higher in CMV patients at 6 months (Fig. 5B).

Discussion

In this single center prospective study of children undergoing allogenic HSCT after myeloablative conditioning as treatment for a hematologic malignancy, we found a clear association between overall plasma protein profile, as well as certain specific proteins, and the complication occurrence.

Hierarchical clustering, an inherently unsupervised process, revealed distinctly different protein profiles with regard to the following outcomes: death, relapse, cGVHD, CMV infection, and immune reconstitution. Delayed immune reconstitution is a well known risk factor for HSCT complications[3]. Even though the predictive value and clinical utility of the method are difficult to establish, hierarchical clustering illustrates the difficulties in denoting specific biomarkers for separate complications since the pathophysiologic processes are greatly intertwined. When considering the individual clinical outcomes, these two clusters were the most clearly separated by CMV reactivation status, which is also a risk factor for delayed immune reconstitution. After analyzing how different protein expression levels correlated during the immune reconstitution period, we can conclude that the complication-prone individuals showed a clearly divergent pattern of protein correlations, while the good outcome-associated cluster 1 displayed a more synchronized pattern. This chaotic appearance is, by our interpretation, a representation of dysregulated immune reconstitution in individuals that developed complications. These findings were in line with the protein pair analysis, where a good outcome was associated with a clear abundance of positively correlating protein pairs at 3 and 6 months (supplementary material, Table S4).

Among the significant proteins differing between patients with CMV viremia and those without, the most noticeable change was that of FCRL6 (Fc receptor-like 6, Fig. 4), an immunoregulatory receptor with restricted expression in cytotoxic lymphocytes[16,17]. The

mechanism of action of FCRL6 is largely unknown, but its interaction with HLA-DR molecules led to reduced cytotoxicity of NK cells towards tumor cells similarly to LAG-3, which is a known marker for effector cell exhaustion[18,19]. Hence, FCRL6 has been suggested to be a possibly druggable check-point molecule to reverse the effector cell exhaustion. It could also serve as a potential biomarker for relapses[18]. To our knowledge, no association between FCRL6 expression and CMV infection has been shown before. While FCRL6 has been shown to be upregulated in chronic inflammatory states[20], we found no connection with e.g. cGVHD or other viral infections. The difference in FCRL6 levels was not explained by standard lymphocyte cell counts, since its expression is restricted to cytotoxic CD8+ and NK cells which showed comparable immune reconstitution between clusters 1 and 2 at the 6 month time point. Since the FCRL6 has no known soluble function, its measurable plasma levels are likely due to increased receptor shedding from FCRL6 positive cells.

Fraction of FCRL6 expressing CD8+ γδ cells was consistently higher in patients that had CMV reactivation (Fig. 5). γδ T cells have a central role in defense against CMV reactivation post-HSCT, and higher levels are associated with higher survival and lower relapse rates[21]. The important role of CMV control by γδ T cells have also been established in the αβ T cell-depleted haploidentical HSCT setting[22], further indicating the importance of circumventing possible γδ T cell exhaustion.

The higher expression of the inhibitory FCRL6 in patients with CMV reactivation indicates that immunosuppressive mechanism is either a cause, or a result of the infection. Based on our findings of a more complex, non-synchronized proteome among complication-prone patients, we theorize that overzealous and asynchronized immune protein production leads to high expression of inhibitory immune checkpoint molecules such as FRCL6 in cytotoxic cells resulting in insufficient control of latent CMV. In addition to a proposed part in immunotherapy resistance[19] and in Human immunodeficiency virus type 1 immune response[23], our results thus indicate that FCRL6 might also play a part in an insufficient anti-CMV immune response following HSCT. Since FCRL6 was significantly more overexpressed on γδ T cells, this could indicate that γδ exhaustion is linked with CMV reactivation.

Other proteins that were higher in CMV-reactivation patients were KLRD1, IL12RB1 (Interleukin 12 receptor subunit beta 1), CD8A and CCL23. All these molecules are associated with cytotoxic responses, i.e. their elevated levels were not surprising in patients experiencing CMV reactivation. Proinflammatory proteins chemokine CCL3 and metalloproteinase MMP-1 were higher in complication-prone patients. MMP-1, a collagen cleaving protease, is involved in inflammatory diseases such as arthritis[24], ulcerative colitis[25], and chronic obstructive pulmonary disease[26], as well as in HIV-infection[27]. AREG, an autocrine growth factor and a mitogen for astrocytes, Schwann cells and fibroblasts[28], was higher in patients with cGVHD at 3 months post-HSCT, probably reflecting the verified relevance of AREG in aGVHD[29] and late aGVHD[30]. Other cGVHD-associations were higher levels of OPG (Osteoprotegerin or TNF receptor superfamily member 11b) and lower levels of CLEC4A.

The relatively small sample size of our cohort did not allow for division into training and validation groups, but our setup with multiple time point measurements in addition to great sample coverage, make the data robust. Ideally, time points would have been more numerous and closer to each other, yielding yet greater information on sequence of events as well as more power to time-dependent analyses. Even though not a weakness per se, our multiple parameter data was under significant strain of multiple testing correction, which might have masked some meaningful true associations.

The classical “one-at-a-time” way of thinking of biomarkers as individual parameters may be challenged by the data mining approaches. For example, a machine learning algorithm has outperformed the EBMT (European Society for Blood and Marrow Transplantation) risk score[31]. Furthermore, biomarker studies are inherently strained by confounding factors[2]. In our study, some individual biomarker analyses could show association with relapse and death, but every single case of relapse or death were found in the same cluster based on the hierarchical clustering approach utilizing the whole protein profile - suggesting that system level analysis outperforms the use of single biomarkers in associating to, and possibly even predicting, major outcomes. Systems immunology is in its infancy[10], but our results indicate

that future studies with larger patient numbers, allowing for division of the cohort into training and validation sets, could reveal signature patterns translatable to the clinic setting.

Acknowledgements

We thank research nurse Pia Valle, and lab technicians Marjo Rissanen, Tamas Bazsinka and Turku University for indispensable assistance.

Authorship Contributions

AA applied for ethics committee approval, collected patient data, planned analyses and wrote the manuscript. MV performed statistical analyses, made the figures and wrote the manuscript. NH performed flow cytometry analysis and wrote the manuscript. XH performed flow cytometry analysis and wrote the manuscript. MT planned the cohort and wrote the manuscript. PH collected patient data and wrote the manuscript. LE supervised and controlled the statistical analyses and wrote the manuscript. MK planned the cohort, acquired funding and wrote the manuscript. EK planned the experiments, supervised the project, acquired funding and wrote the manuscript.

References

1. Wingard JR, Majhail NS, Brazauskas R, et al. Long-term survival and late deaths after allogeneic hematopoietic cell transplantation. *J Clin Oncol*. 2011;29(16):2230-2239.

2. Adom D, Rowan C, Adeniyan T, Yang J, Paczesny S. Biomarkers for Allogeneic HCT Outcomes. *Front Immunol*. 2020;11:673.

3. de Koning C, Plantinga M, Besseling P, Boelens JJ, Nierkens S. Immune Reconstitution after Allogeneic Hematopoietic Cell Transplantation in Children. *Biol Blood Marrow Transplant*. 2016;22(2):195-206.

4. Blennow O, Ljungman P, Sparrelid E, Mattsson J, Remberger M. Incidence, risk factors, and outcome of bloodstream infections during the pre-engraftment phase in 521 allogeneic hematopoietic stem cell transplantations. *Transpl Infect Dis*. 2014;16(1):106-114.

5. Zhang P, Jiang EL, Yang DL, et al. Risk factors and prognosis of invasive fungal infections in allogeneic stem cell transplantation recipients: a single-institution experience. *Transpl Infect Dis*. 2010;12(4):316-321.

6. Stern L, Withers B, Avdic S, et al. Human Cytomegalovirus Latency and Reactivation in Allogeneic Hematopoietic Stem Cell Transplant Recipients. *Front Microbiol*. 2019;10:1186.

7. Camargo JF, Wieder ED, Kimble E, et al. Deep functional immunophenotyping predicts risk of cytomegalovirus reactivation after hematopoietic cell transplantation. *Blood*. 2019;133(8):867-877.

8. Chen S, Zeiser R. Novel Biomarkers for Outcome After Allogeneic Hematopoietic Stem Cell Transplantation. *Front Immunol*. 2020;11:1854.

9. Giaccone L, Faraci DG, Butera S, et al. Biomarkers for acute and chronic graft versus host disease: state of the art. *Expert Rev Hematol*. Published online December 24, 2020:1-18.

10. Davis MM. Systems immunology. *Curr Opin Immunol*. 2020;65:79-82.

11. Alexandersson A, Koskenvuo M, Tiderman A, et al. Viral infections and immune reconstitution interaction after pediatric allogenic hematopoietic stem cell transplantation. *Infect Dis*. 2019;51(10):772-778.

12. Jagasia MH, Greinix HT, Arora M, et al. National Institutes of Health Consensus Development Project on Criteria for Clinical Trials in Chronic Graft-versus-Host Disease:

I. The 2014 Diagnosis and Staging Working Group Report. *Biol Blood Marrow Transplant*. 2015;21(3):389-401.e1.

13. Glucksberg H, Storb R, Fefer A, et al. CLINICAL MANIFESTATIONS OF GRAFT-VERSUS-HOST DISEASE IN HUMAN RECIPIENTS OF MARROW FROM HL-A-MATCHED SIBLING DONOR,S. *Transplantation*. 1974;18(4):295.

14. Assarsson E, Lundberg M, Holmquist G, et al. Homogenous 96-plex PEA immunoassay exhibiting high sensitivity, specificity, and excellent scalability. *PLoS One*. 2014;9(4):e95192.

15. Conesa A, Nueda MJ, Ferrer A, Talón M. maSigPro: a method to identify significantly differential expression profiles in time-course microarray experiments. *Bioinformatics*. 2006;22(9):1096-1102.

16. Schreeder DM, Cannon JP, Wu J, Li R, Shakhmatov MA, Davis RS. Cutting edge: FcR-like 6 is an MHC class II receptor. *J Immunol*. 2010;185(1):23-27.

17. Kulemzin SV, Zamoshnikova AY, Yurchenko MY, et al. FCRL6 receptor: expression and associated proteins. *Immunol Lett*. 2011;134(2):174-182.

18. Davis RS. Roles for the FCRL6 Immunoreceptor in Tumor Immunology. *Front Immunol*. 2020;11:575175.

19. Johnson DB, Nixon MJ, Wang Y, et al. Tumor-specific MHC-II expression drives a unique pattern of resistance to immunotherapy via LAG-3/FCRL6 engagement. *JCI Insight*. 2018;3(24). doi:10.1172/jci.insight.120360

20. Schreeder DM, Pan J, Li FJ, Vivier E, Davis RS. FCRL6 distinguishes mature cytotoxic lymphocytes and is upregulated in patients with B-cell chronic lymphocytic leukemia. *Eur J Immunol*. 2008;38(11):3159-3166.

21. Arruda LCM, Gaballa A, Uhlin M. Impact of γδ T cells on clinical outcome of

hematopoietic stem cell transplantation: systematic review and meta-analysis. *Blood Adv*. 2019;3(21):3436-3448.

22. Park M, Im HJ, Lee YJ, et al. Reconstitution of T and NK cells after haploidentical hematopoietic cell transplantation using αβ T cell-depleted grafts and the clinical implication of γδ T cells. *Clin Transplant*. 2018;32(1):e13147.

23. Wilson TJ, Presti RM, Tassi I, Overton ET, Cella M, Colonna M. FcRL6, a new ITIM-bearing receptor on cytolytic cells, is broadly expressed by lymphocytes following HIV-1 infection. *Blood*. 2007;109(9):3786-3793.

24. Burrage PS, Mix KS, Brinckerhoff CE. Matrix metalloproteinases: role in arthritis. *Front Biosci*. 2006;11:529-543.

25. Wang YD, Yan PY. Expression of matrix metalloproteinase-1 and tissue inhibitor of metalloproteinase-1 in ulcerative colitis. *World J Gastroenterol*. 2006;12(37):6050-6053.

26. Montaño M, Sansores RH, Becerril C, et al. FEV1 inversely correlates with metalloproteinases 1, 7, 9 and CRP in COPD by biomass smoke exposure. *Respir Res*. 2014;15(1):74.

27. Rumbaugh J, Turchan-Cholewo J, Galey D, et al. Interaction of HIV Tat and matrix metalloproteinase in HIV neuropathogenesis: a new host defense mechanism. *FASEB J*. 2006;20(10):1736-1738.

28. Uhlén M, Karlsson MJ, Hober A, et al. The human secretome. *Sci Signal*. 2019;12(609). doi:10.1126/scisignal.aaz0274

29. Holtan SG, DeFor TE, Panoskaltsis-Mortari A, et al. Amphiregulin modifies the Minnesota Acute Graft-versus-Host Disease Risk Score: results from BMT CTN 0302/0802. *Blood Adv*. 2018;2(15):1882-1888.

30. Holtan SG, Khera N, Levine JE, et al. Late acute graft-versus-host disease: a

prospective analysis of clinical outcomes and circulating angiogenic factors. *Blood*. 2016;128(19):2350-2358.

31. Shouval R, Labopin M, Bondi O, et al. Prediction of Allogeneic Hematopoietic Stem-Cell Transplantation Mortality 100 Days After Transplantation Using a Machine Learning Algorithm: A European Group for Blood and Marrow Transplantation Acute Leukemia Working Party Retrospective Data Mining Study. *Journal of Clinical Oncology*. 2015;33(28):3144-3151. doi:10.1200/jco.2014.59.1339

Figures legends

Table 1. Cohort demographics. MUD, matched unrelated donor; ALL, acute lymphoblastic leukemia; CML, chronic myeloid leukemia; NHL, non-Hodgkin lymphoma; AML, acute myeloid leukemia; MDS, myelodysplastic syndrome; MPAL, mixed phenotype acute leukemia; TBI, total body irradiation; GVHD, graft-versus-host disease. Serotherapy: Alemtuzumab or anti-thymocyte globulin. *Differences between complication-free and complication-prone groups were tested using the Mann–Whitney test for continuous variables (age) and the chi-squared test or Fisher's exact test (N < 5) for categorical variables.

Fig. 1. Trajectories of individual proteins. Spark-line plot of protein kinetics over time according to patient grouping by complication-free status (see methods for definition). Highlighted proteins were found to be clearly associated with complications.

Fig. 2. Protein profile in relation to outcome. A Heatmap generated by hierarchical clustering of protein levels at 6 months post-HSCT. One patient per row is displayed, with patient characteristics to the left. **B** Comparison of immune reconstitution between the two major clusters from the heatmap. The p values were obtained for cluster×time interaction

terms in linear mixed effect models with time and cluster as additional fixed effects and including a random intercept for patients.

Fig. 3. Inter-protein correlations within complication-free and complication-prone groups. A Histograms of Pearson's correlation coefficients grouped according to complication status. **B** Pearson's correlation matrices for correlation-free and correlation-prone groups. The proteins were ordered according to the differences in correlation between the two groups by the median strength of correlation differences for each protein.

Fig. 4 Individual proteins and outcomes. A Kinetics of maSigPro-identified significant protein level differences over time, depending on outcome. One line represents one patient. **B** Timepoint specific comparison of protein levels depending on CMV status. **C** Levels of differentiation according to outcome and timepoint depending on CMV status. **D** Timepoint specific comparison of protein levels depending on complication status. **E** Levels of differentiation according to outcome and timepoint depending on complication status. FCRL6, Fc receptor-like protein 6; CLEC4A, C-type lectin domain family 4 member A; AREG, Amphiregulin; OPG, Osteoprotegerin;; CCL23, C-C motif chemokine ligand 23; KLRD1, Killer cell lectin like receptor D1; IL12RB1, Interleukin 12 receptor subunit beta 1; CD8A, T-cell surface glycoprotein CD8 alpha chain; MMP-1, Matrix metalloproteinase-1; CCL3, C-C motif chemokine 3.

Fig. 5. FCRL6-positive cytotoxic T cell subsets in patients with CMV viremia. A The box plots show the fraction of FCRL6+ cells of CD8+ T cells, CD8+ central memory T cells, CD8+ effector memory T cells and CD8+ effector memory RA+ T cells at different time points, depending on CMV status. **B** The box plots show the fraction of FCRL6+ cells of all γδ T cells and of CD8+ γδ T cells, depending on CMV status.

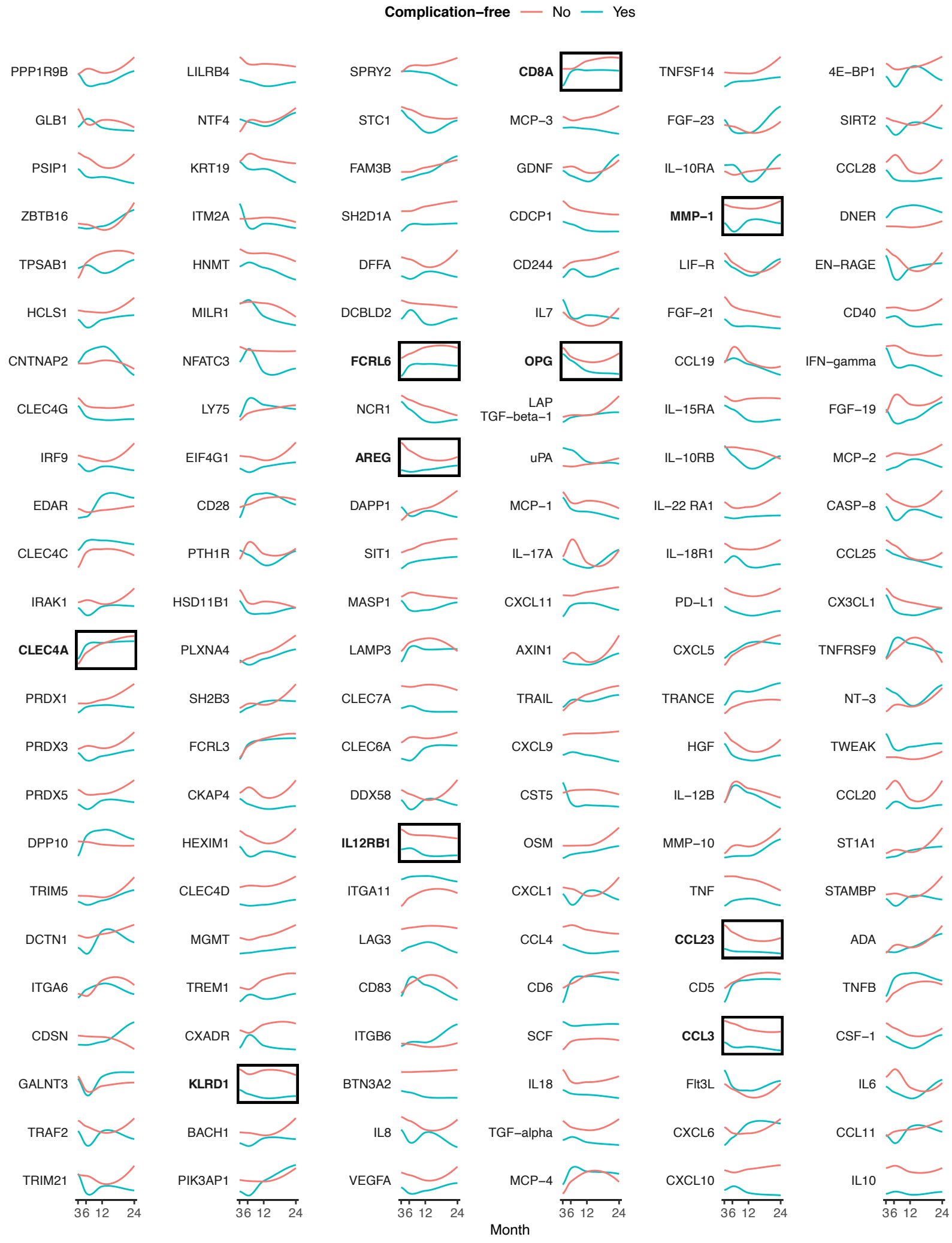

Fig. 1. Trajectories of individual proteins. Spark-line plot of protein kinetics over time according to patient grouping by complication-free status (see methods for definition). Highlighted proteins were found to be clearly associated with complications.

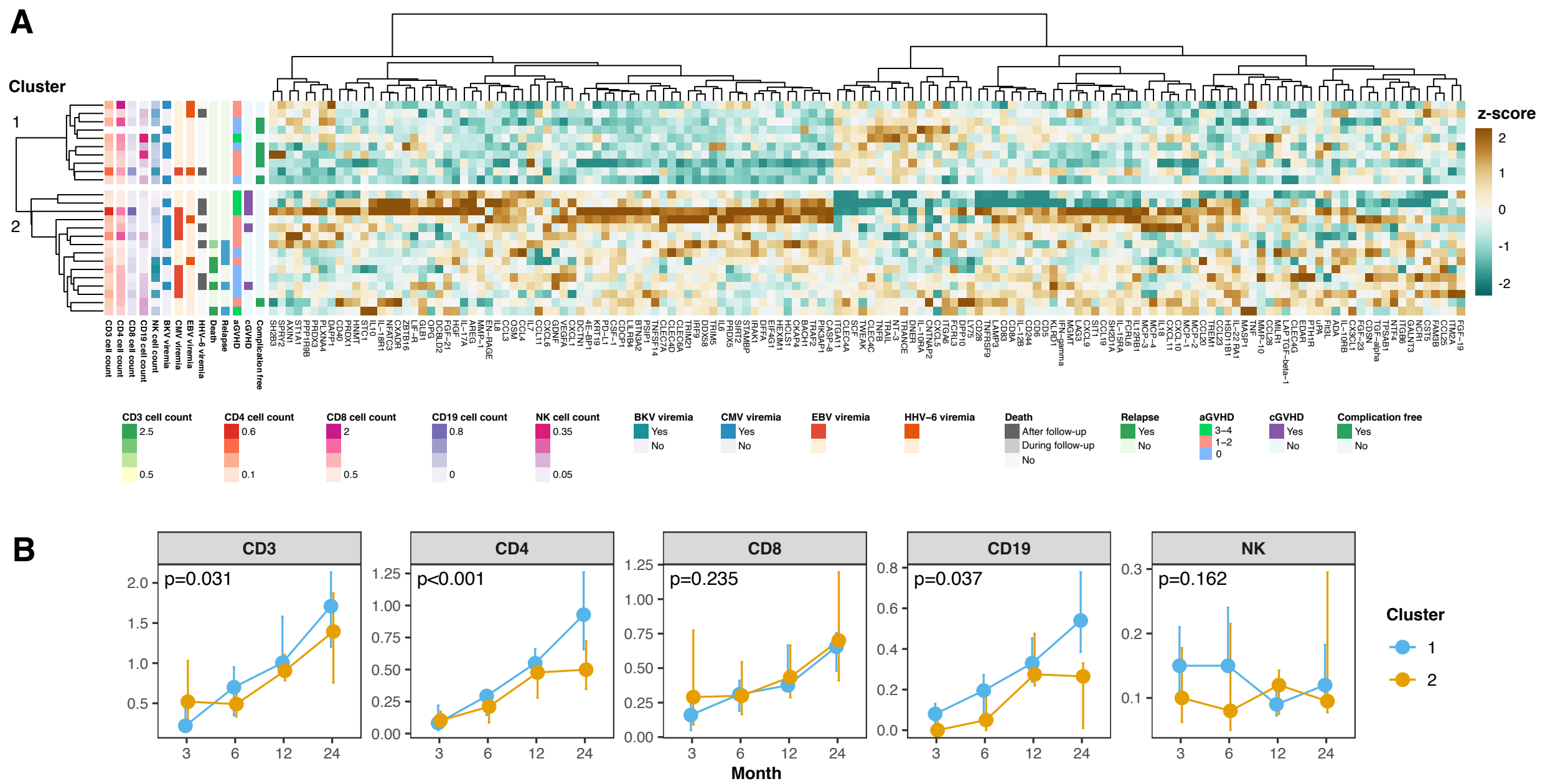

Fig. 2. Protein profile in relation to outcome. **A** Heatmap generated by hierarchical clustering of protein levels at 6 months post-HSCT. One patient per row is displayed, with patient characteristics to the left. **B** Comparison of immune reconstitution between the two major clusters from the heatmap. The p values were obtained for cluster×time interaction terms in linear mixed effect models with time and cluster as additional fixed effects and including a random

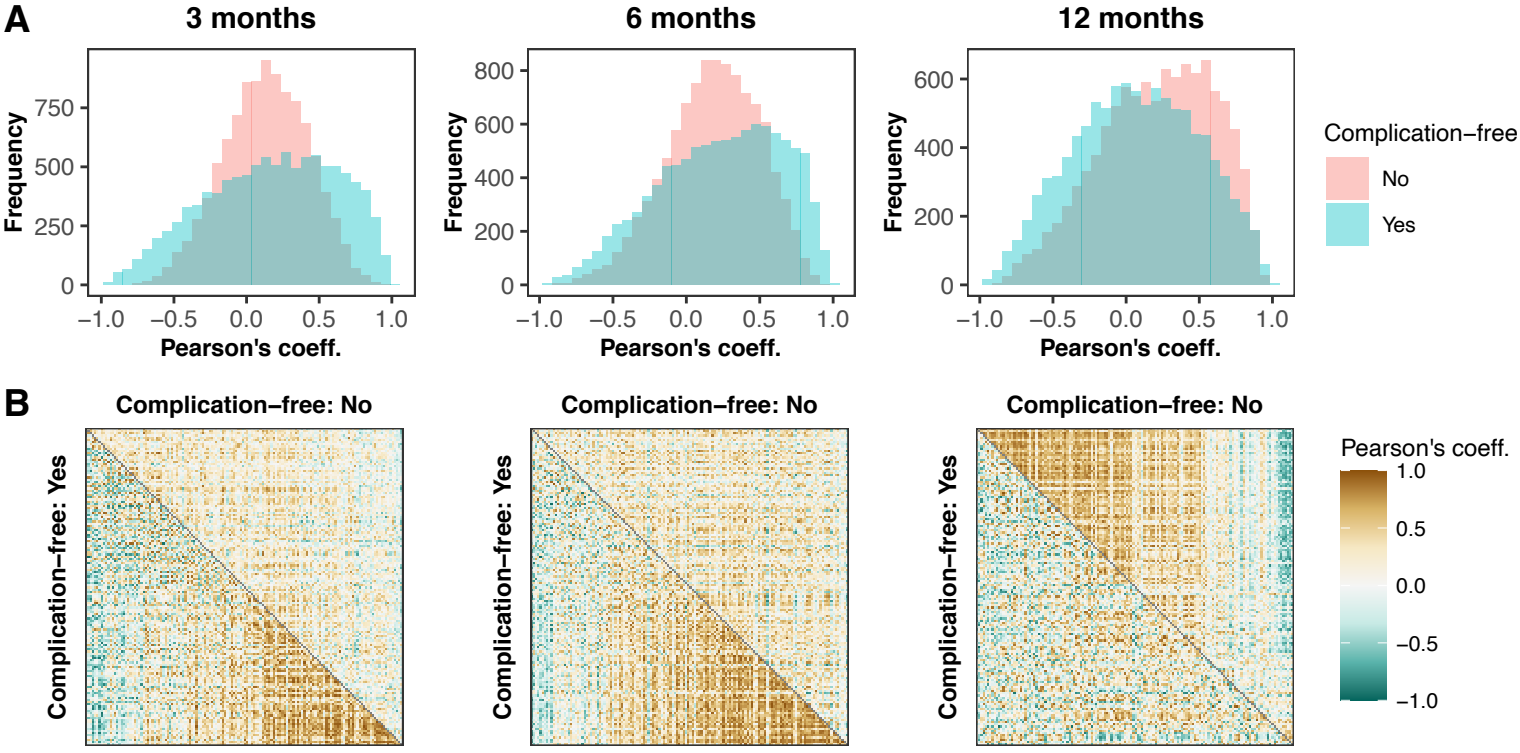

Fig. 3. Inter-protein correlations within complication-free and complication-prone groups. **A** Histograms of Pearson's correlation coefficients grouped according to complication status. **B** Pearson's correlation matrices for correlation-free and correlation-prone groups. The proteins were ordered according to the differences in correlation between the two groups by the median strength of correlation differences for each protein.

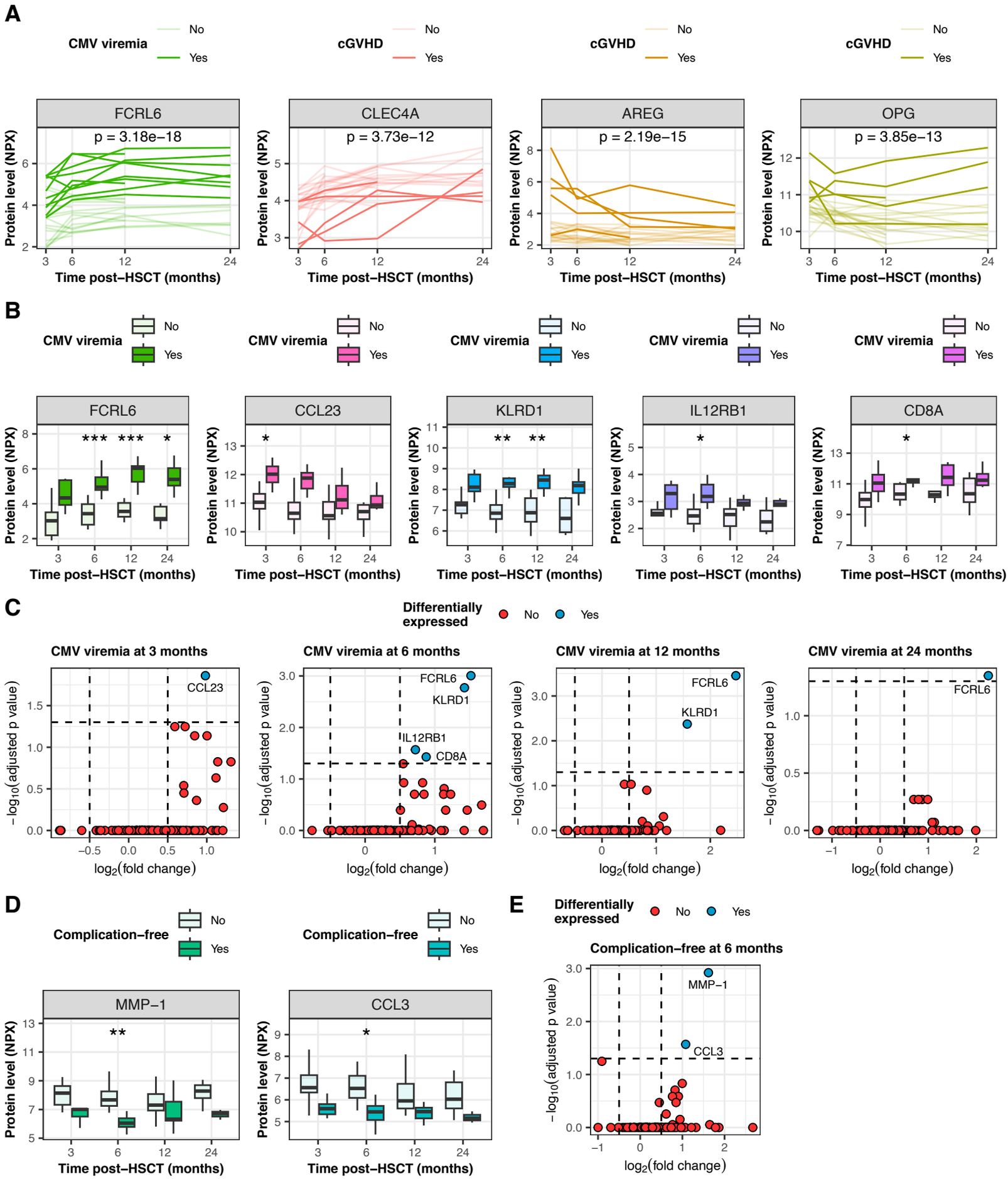

Fig. 4 Individual proteins and outcomes. **A** Kinetics of maSigPro-identified significant protein level differences over time, depending on outcome. One line represents one patient. **B** Timepoint specific comparison of protein levels depending on CMV status. **C** Levels of differentiation according to outcome and timepoint depending on CMV status. **D** Timepoint specific comparison of protein levels depending on complication status. **E** Levels of differentiation according to outcome and timepoint depending on complication status. FCRL6, Fc receptor-like protein 6; CLEC4A, C-type lectin domain family 4 member A; AREG, Amphiregulin; OPG, Osteoprotegerin;; CCL23, C-C motif chemokine ligand 23; KLRD1, Killer cell lectin like receptor D1; IL12RB1, Interleukin 12 receptor subunit beta 1; CD8A, T-cell surface glycoprotein CD8 alpha chain; MMP-1, Matrix metalloproteinase-1; CCL3, C-C motif chemokine 3.

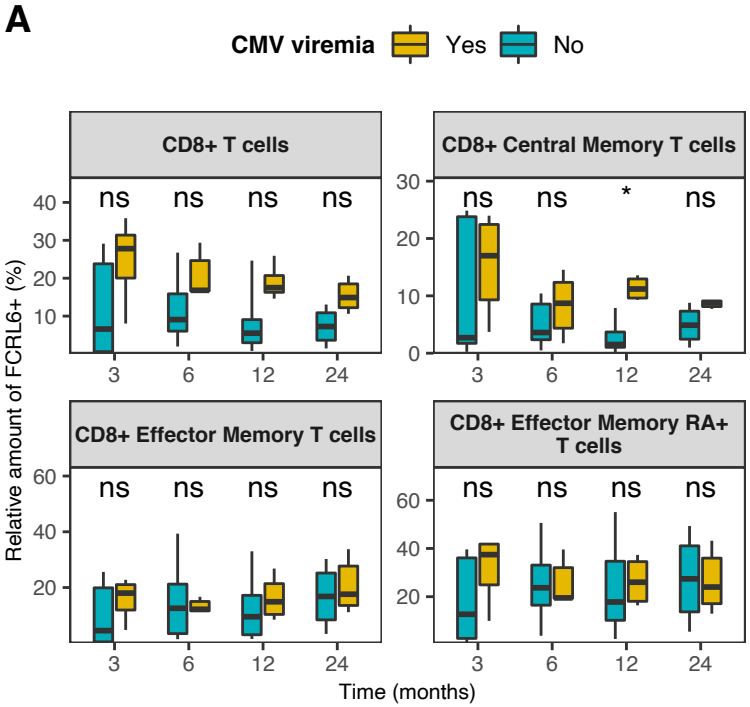

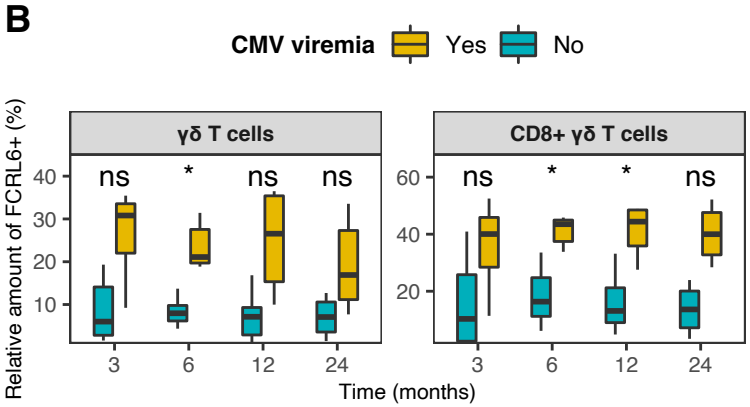

Fig. 5. FCRL6-positive cytotoxic T cell subsets in patients with CMV viremia. **A** The box plots show the fraction of FCRL6+ cells of CD8+ T cells, CD8+ central memory T cells, CD8+ effector memory T cells and CD8+ effector memory RA+ T cells at different time points, depending on CMV status. **B** The box plots show the fraction of FCRL6+ cells of all γδ T cells and of CD8+ γδ T cells, depending on CMV status.

Supplementary material

Quality control and descriptive statistics

All 90 samples of the 27 patients collected at time points 3, 6, 12 and 24 months post-HSCT passed Olink quality control, yielding a total of 16560 measurements excluding technical controls. Values below the validated limit of detection (LOD) ranged from 0% to 94% per protein, with 20% of proteins having more than 50% of measurements below LOD. We performed statistical analyses separately both with and without values below LOD, and no relevant or noticeable differences were found when comparing results presented with or without values below LOD. Therefore, presented results are based on actual data, including values below LOD. Four individual proteins were included in both panels used. To avoid their overrepresentation, only the proteins from panels containing fewer values below LOD were used in downstream analyses. Results of the shared proteins showed good correlation between panels (supplementary material, Fig. S3), further providing evidence of good technical quality of the data obtained.

Table S1. Proteins measured with Proximity Extension Assay.

Inflammation panel		Immune response panel	
IL8	IL-15RA	PPP1R9B	PLXNA4
VEGFA	IL-10RB	GLB1	SH2B3
CD8A	IL-22 RA1	PSIP1	FCRL3
MCP-3	IL-18R1	ZBTB16	CKAP4
GDNF	PD-L1	IRAK4	JUN
CDCP1	Beta-NGF	TPSAB1	HEXIM1
CD244	CXCL5	HCLS1	CLEC4D
IL7	TRANCE	CNTNAP2	PRKCQ
OPG	HGF	CLEC4G	MGMT
LAP TGF-beta-1	IL-12B	IRF9	TREM1
uPA	IL-24	EDAR	CXADR
IL6	IL13	IL6	IL10
IL-17C	ARTN	DGKZ	SRPK2
MCP-1	MMP-10	CLEC4C	KLRD1
IL-17A	IL10	IRAK1	BACH1
CXCL11	TNF	CLEC4A	PIK3AP1
AXIN1	CCL23	PRDX1	SPRY2
TRAIL	CD5	PRDX3	STC1
IL-20RA	CCL3	FGF2	ARNT
CXCL9	Flt3L	PRDX5	FAM3B
CST5	CXCL6	DPP10	SH2D1A
IL-2RB	CXCL10	TRIM5	ICA1
IL-1 alpha	4E-BP1	DCTN1	DFFA
OSM	IL-20	ITGA6	DCBLD2
IL2	SIRT2	CDSN	FCRL6
CXCL1	CCL28	GALNT3	NCR1
TSLP	DNER	FXYD5	CXCL12
CCL4	EN-RAGE	TRAF2	AREG
CD6	CD40	TRIM21	IFNLR1
SCF	IL33	LILRB4	DAPP1
IL18	IFN-gamma	NTF4	PADI2
SLAMF1	FGF-19	KRT19	SIT1
TGF-alpha	IL4	ITM2A	MASP1
MCP-4	LIF	HNMT	LAMP3
CCL11	NRTN	CCL11	CLEC7A
TNFSF14	MCP-2	MILR1	CLEC6A
FGF-23	CASP-8	EGLN1	DDX58
IL-10RA	CCL25	NFATC3	IL12RB1
FGF-5	CX3CL1	LY75	TANK
MMP-1	TNFRSF9	EIF5A	ITGA11
LIF-R	NT-3	EIF4G1	KPNA1
FGF-21	TWEAK	CD28	LAG3
CCL19	CCL20	PTH1R	IL5
ADA	ST1A1	BIRC2	CD83
TNFB	STAMBP	HSD11B1	ITGB6
CSF-1	IL5	NF2	BTN3A2

Table S2. Available samples per patient and time point for flow cytometry.

	3 months	6 months	12 months	24 months
P3	x	x	x	x
P8	x			
P11	x		x	x
P5		x	x	x
P20	x			
P13	x			
P16	x		x	x
P17	x	x	x	
P19	x	x	x	
P21	x	x	x	
P23	x	x	x	
P22		x	x	x
P6	x	x	x	
P7	x	x	x	
P24	x	x	x	
P26	x	x	x	
P9	x	x		

Table S3. Fluorescent-labeled anti-human antibodies used in flow cytometry analysis.

Antibody	Clone	Producer	Concentration
CD19-FITC	HI19a	Immunotools	1 : 50
CD14-FITC	18D11	Immunotools	1 : 50
CD8-PE	MEM-31	Immunotools	1 : 100
CCR7 (CD197)-PE-CF594	150503	BD Biosciences	1 : 20
CD31-PeCy7	WM59	BD Biosciences	1 : 100
FCRL6-APC	7B7/FcRL6	BioLegend	1 : 50
CD28-AlexaFluor700	CD28.2	BD Biosciences	1 : 10
CD3-APC-H7	SK7	BD Biosciences	1 : 50
CD95 (FAS)-BV421	DX2	BD Biosciences	1 : 100
CD4-BV510	SK3	BD Biosciences	1 : 50
TCRgd-BV605	11F2	BD Biosciences	1 : 100
CD21-BV650	B-ly4	BD Biosciences	1 : 20
CD45RA-BV711	HI100	BD Biosciences	1 : 50

Fig. S1. Gating strategy of FCRL6 expression in T cell subsets. The red dots in SSC-H versus FCRL6-APC plots show FCLR6 expression in a representative donor, and the blue dots show the fluorescence-minus-one sample.

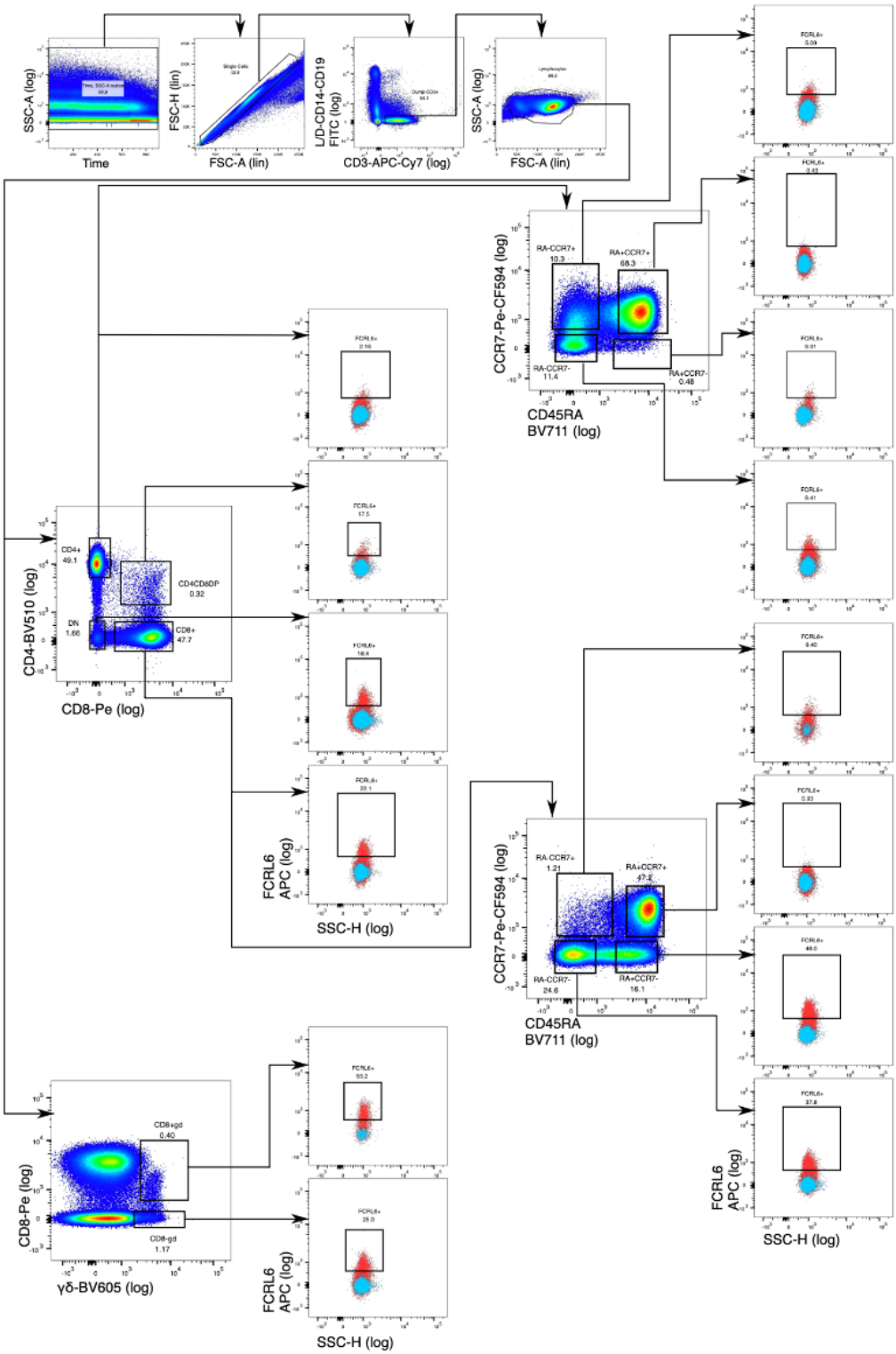

Fig. S2. PCA according to outcomes cGVHD, death, relapse and complication status.

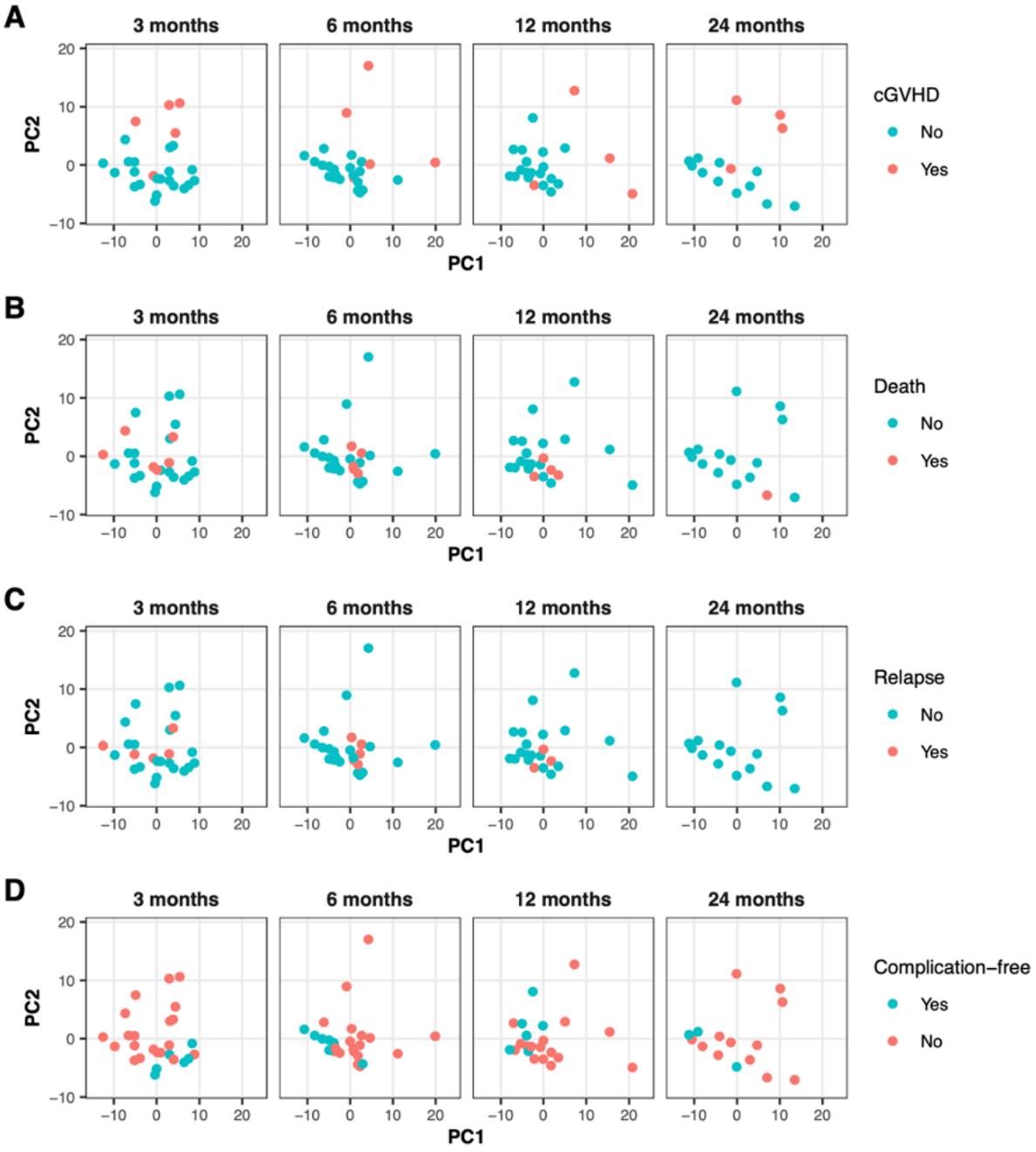

Fig. S3. Inflammation-Immune response-panel correlation.

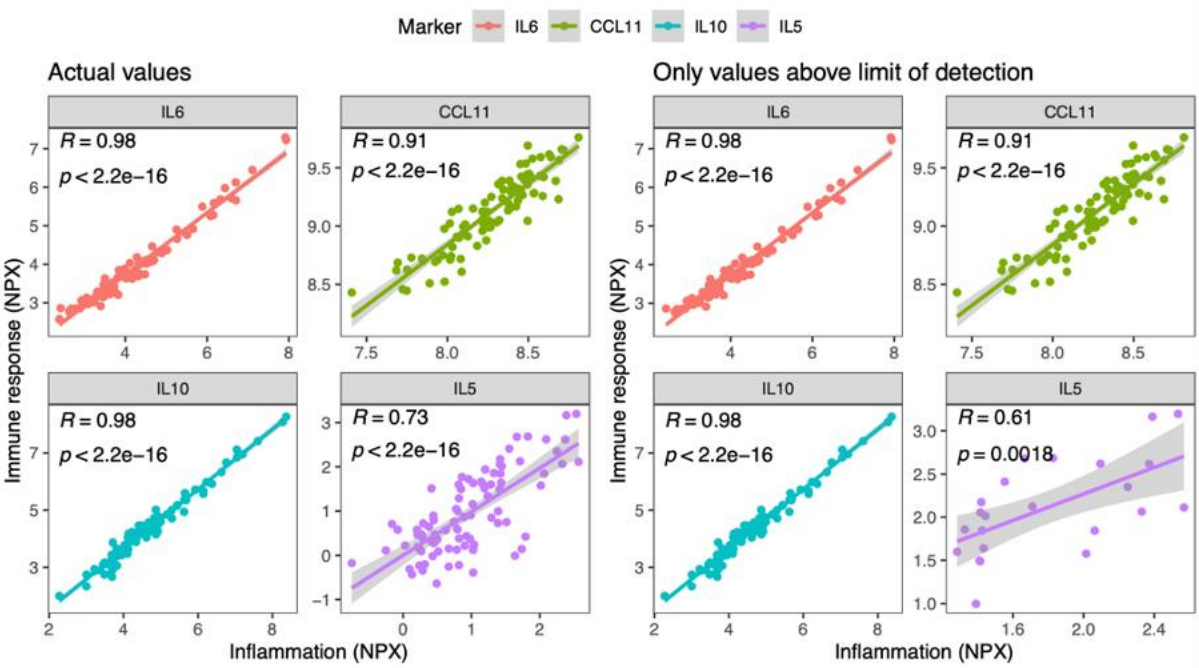

Fig. S4. Heatmaps at time points 3, 6, 12 and 24 months post-HSCT.

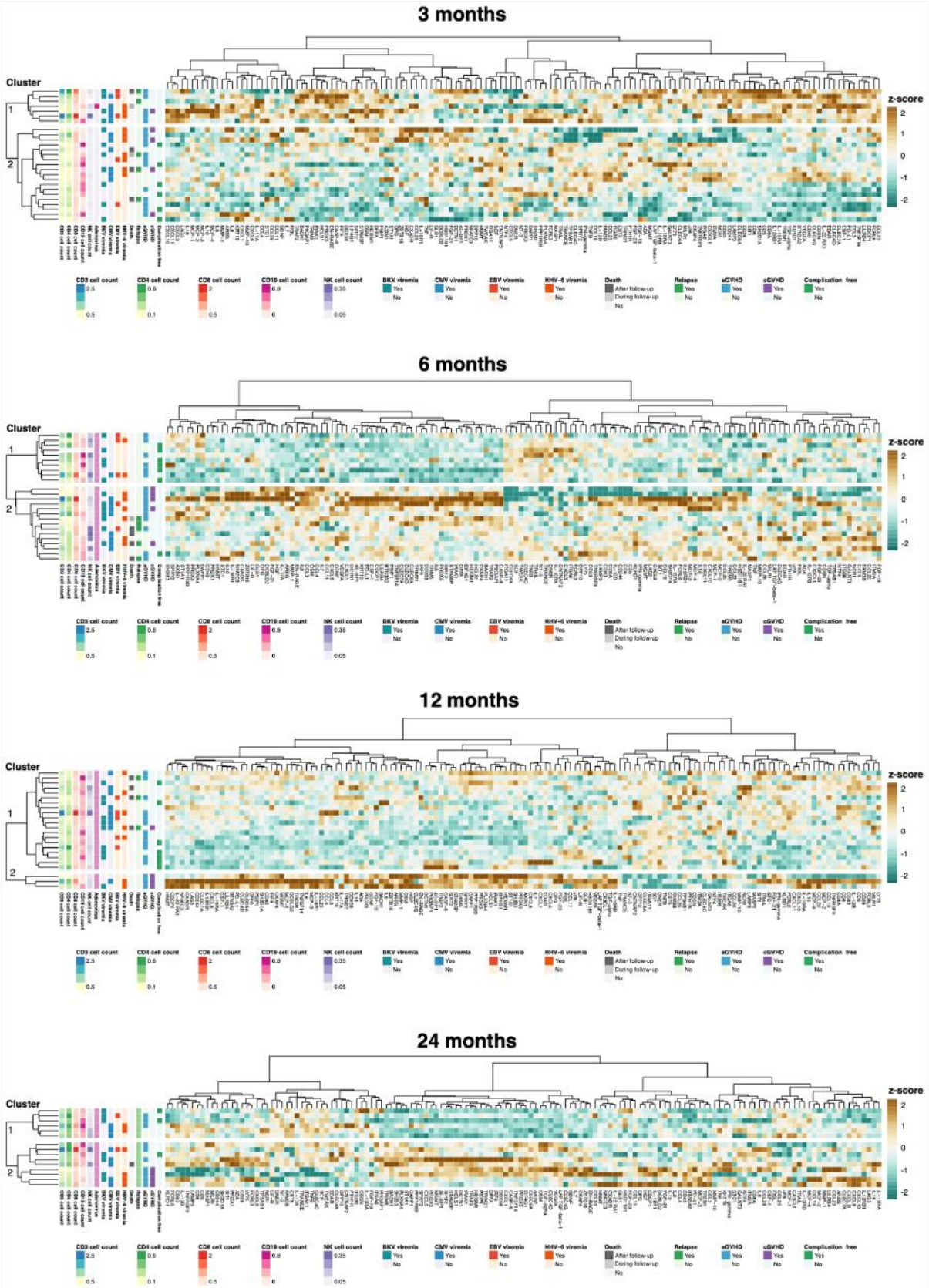

Table S4. Differentially correlating protein pairs between complication-free and complication-prone groups. Type of difference: +/0 = high correlation in complication-free group and low in complication-prone, etc.

	Differences in inter-protein correlation									
Timepoint	Protein 1	Protein 2	Inter-protein correlation in complication-free group	p value for inter-protein correlation in complication-free group	Inter-protein correlation in complication-prone group	p value for inter-protein correlation in complication-prone group	z statistic for difference in correlations between groups	p value for inter-group differences in correlation	Adjusted p value for inter-group differences in correlation	Type of correlation difference
3	DCBLD2	ITGB6	0,9766324	0,0008127	-0,2939212	0,2084543	-4,0269171	0,0000565	0,0056513	+/0
3	CLEC4A	HSD11B1	0,9927543	0,0000786	0,1505960	0,5262433	-3,9840393	0,0000678	0,0067754	+/0
3	AREG	MASP1	0,8977057	0,0151610	-0,7636461	0,0000893	-3,9365729	0,0000827	0,0082654	+/-
3	GLB1	TNFRSF9	0,9823281	0,0004657	-0,0990965	0,6776566	-3,9274225	0,0000859	0,0085861	+/0
3	LY75	CCL25	0,9742111	0,0009890	-0,1366937	0,5655219	-3,6832560	0,0002303	0,0230274	+/0
3	PTH1R	BTN3A2	0,9877850	0,0002229	0,2664190	0,2562009	-3,6297732	0,0002837	0,0283670	+/0
3	SCF	IL-15RA	0,9500052	0,0036867	-0,4018573	0,0790277	-3,6052522	0,0003119	0,0311850	+/0
3	Flt3L	CCL28	0,9618950	0,0021503	-0,2399909	0,3081277	-3,5377493	0,0004036	0,0403553	+/0
3	CD40	NT-3	0,9642376	0,0018956	-0,1779695	0,4528452	-3,4857574	0,0004907	0,0490746	+/0
6	HEXIM1	IL-17A	-0,9230028	0,0030303	0,7944506	0,0000822	4,7843798	0,0000017	0,0001715	-/+
6	CD83	IL8	0,9792901	0,0001172	-0,2185183	0,3836804	-4,4462422	0,0000087	0,0008739	+/0
6	IL8	IL-17A	-0,8876081	0,0076494	0,7610014	0,0002448	4,2811308	0,0000186	0,0018595	-/+
6	ZBTB16	IL6	0,9921548	0,0000104	0,3277422	0,1842795	-4,0985019	0,0000416	0,0041583	+/0
6	FCRL3	LIF-R	0,9704360	0,0002841	-0,1915851	0,4463169	-4,0760284	0,0000458	0,0045811	+/0
6	AREG	CCL25	0,9511280	0,0009877	-0,4128865	0,0885828	-4,0562247	0,0000499	0,0049872	+/0
6	TRAF2	LY75	0,9682974	0,0003379	-0,1561878	0,5359864	-3,9481345	0,0000788	0,0078763	+/0
6	Flt3L	FGF-19	-0,9655945	0,0004140	0,1943852	0,4395716	3,9442572	0,0000800	0,0080048	-/0
6	EIF4G1	IL-17A	-0,8991039	0,0058783	0,6249511	0,0055525	3,9105887	0,0000921	0,0092071	-/+
6	TGF-alpha	CCL23	0,9890126	0,0000242	0,3977511	0,1021260	-3,8710292	0,0001084	0,0108377	+/0
6	KLRD1	BACH1	0,9682689	0,0003386	-0,0731676	0,7729452	-3,7977345	0,0001460	0,0146025	+/0
6	LY75	IL8	0,9467042	0,0012237	-0,2494982	0,3180636	-3,6498683	0,0002624	0,0262375	+/0
6	LY75	PTH1R	0,9784906	0,0001288	0,2354290	0,3469895	-3,5911818	0,0003292	0,0329182	+/0
6	PRDX1	TRIM21	0,9870367	0,0000365	0,4658235	0,0513772	-3,5743783	0,0003511	0,0351061	+/0
12	CXADR	IL-18R1	-0,8535967	0,0145342	0,9021739	0,0000018	4,8149266	0,0000015	0,0001473	-/+
12	OPG	FGF-21	-0,9708000	0,0002755	0,4367244	0,0907686	4,5021254	0,0000067	0,0006728	-/0
12	IL-22 RA1	HGF	-0,9470148	0,0012061	0,5815716	0,0181244	4,3144025	0,0000160	0,0016004	-/+
12	LIF-R	IL-22 RA1	-0,9182044	0,0035154	0,6836510	0,0035002	4,2209106	0,0000243	0,0024332	-/+
12	CXADR	DFFA	-0,8086293	0,0276759	0,8473668	0,0000342	4,1446521	0,0000340	0,0034033	-/+
12	KRT19	IL-15RA	0,9707081	0,0002776	-0,2501330	0,3501268	-4,1274745	0,0000367	0,0036677	+/0
12	MCP-2	IL6	-0,8849299	0,0081012	0,7262953	0,0014419	4,0556279	0,0000500	0,0050000	-/+
12	LILRB4	CASP-8	-0,8829357	0,0084474	0,7249876	0,0014851	4,0348461	0,0000546	0,0054638	-/+
12	TNFSF14	DNER	0,9080823	0,0046798	-0,6376990	0,0078695	-3,9714546	0,0000714	0,0071435	+/-
12	DPP10	LIF-R	-0,9460043	0,0012638	0,4405365	0,0876669	3,9617386	0,0000744	0,0074406	-/0
12	NFATC3	SCF	0,8450761	0,0166617	-0,7704381	0,0004788	-3,9527577	0,0000773	0,0077256	+/-
12	LILRB4	PIK3AP1	-0,8350469	0,0193802	0,7820230	0,0003445	3,9441246	0,0000801	0,0080092	-/+
12	EDAR	CXCL5	0,9890208	0,0000241	0,3382168	0,2000917	-3,9309720	0,0000846	0,0084603	+/0
12	MCP-1	TWEAK	0,9243533	0,0029013	-0,5508657	0,0270028	-3,9137273	0,0000909	0,0090882	+/-
12	DCBLD2	LAG3	-0,8953383	0,0064288	0,6521970	0,0061802	3,8954734	0,0000980	0,0098007	-/+
12	IL8	CD40	-0,7157060	0,0705196	0,8611088	0,0000184	3,8413987	0,0001223	0,0122335	0/+